Check for updates

ADVANCED MATERIALS
www.advmat.de

Tailoring the Coordination Micro-Environment in Nanotraps for Efficient Platinum/Palladium Separation

*Yanpei Song, Gaurav Verma, Kui Tan, Kolade A Oyekan, Juejing Liu, Andrew Strzelecki, Xiaofeng Guo, Abdullah M. Al-Enizi, Ayman Nafady, and Shengqian Ma**

Recovering platinum group metals from secondary resources is crucial to meet the growing demand for high-tech applications. Various techniques are explored, and adsorption using porous materials has emerged as a promising technology due to its efficient performance and environmental beingness. However, the challenge lies in effectively recovering and separating individual platinum group metals (PGMs) given their similar chemical properties. Herein, a breakthrough approach is presented by sophisticatedly tailoring the coordination micro-environment in a series of aminopyridine-based porous organic polymers, which enables the creation of platinum-specific nanotraps for efficient separation of binary PGMs (platinum/palladium). The newly synthesized POP-*o*2NH$_2$-Py demonstrates record uptakes and selectivity toward platinum over palladium, with the amino groups adjacent to the pyridine moieties being vital in improving platinum binding performance. Further breakthrough experiments underline its remarkable ability to separate platinum and palladium. Spectroscopic analysis reveals that POP-*o*2NH$_2$-Py offers a more favorable coordination fashion to platinum ions compared to palladium ions owing to the greater interaction between N and Pt^{4+} and stronger intramolecular hydrogen bonding between the amino groups and four coordinating chlorines at platinum. These findings underscore the importance of fine-tuning the coordination micro-environment of nanotraps through subtle modifications that can greatly enhance the selectivity toward the desired metal ions.

1. Introduction

Platinum group metals (PGMs) are the collective name of six noble metallic elements, including platinum (Pt), palladium (Pd), rhodium (Rh), osmium (Os), iridium (Ir) and ruthenium (Ru), which are clustered together in the periodic table and possess distinctive chemical and physical properties, such as excellent electrical conductivity, high catalytical activity, and strong corrosion and oxidation resistance.[1–3] These characteristics make them indispensable in a variety of high-tech applications, including the manufacturing of electronic and electrical devices, catalysts for a range of chemical and electrochemical reactions, fuel cells, medical materials, and chemotherapy medication.[4–7] Among their notable applications, PGMs are highly regarded for their exceptional catalytic properties in automotive catalytic converters, such as Three-Way-Catalyst (TWC), Diesel-Oxidation Catalyst (DOC), Selective Catalytic Reduction.[8] However, the scarcity of PGM ores and the intricate processes involved in mining and refining contribute to the high cost of recovering these precious metals from primary sources. Recycling them from secondary resources has emerged as a technically feasible and cost-effective solution to meet the growing demand for these metals in various industries.[9–12]

Spent automotive catalytic converters are highly valuable secondary resources of PGMs, as their PGM content per unit is significantly higher compared to corresponding mineral ores. The recovery of PGMs from these spent catalysts has gained considerable attention, which is believed as a promising alternative to supplement the declining primary production of PGMs.[13–16] Conventional methods used in recycling industries, such as pyrometallurgy and hydrometallurgy, have already been explored for PGM recovery; and biometallurgical techniques including bioleaching and biosorption, have also been investigated through bench-scale tests.[8] Those techniques, however, often involve hash chemical and physical treatments, which are energy-consuming, environmentally polluting, and expensive. Moreover, spent automotive catalytic converters, such as TWC, typically contain multiple PGMs, which presents a challenge in

Y. Song, G. Verma, K. Tan, S. Ma
Department of Chemistry
University of North Texas
Denton, TX 76201, USA
E-mail: Shengqian.Ma@unt.edu
K. A Oyekan
Department of Materials Science & Engineering
University of Texas at Dallas
Richardson, TX 75080, USA
J. Liu, A. Strzelecki, X. Guo
Department of Chemistry
Washington State University
Pullman, WA 99164, USA
A. M. Al-Enizi, A. Nafady
Department of Chemistry
College of Science
King Saud University
Riyadh 11451, Saudi Arabia

The ORCID identification number(s) for the author(s) of this article can be found under https://doi.org/10.1002/adma.202313747

DOI: 10.1002/adma.202313747

 © 2024 Wiley-VCH GmbH

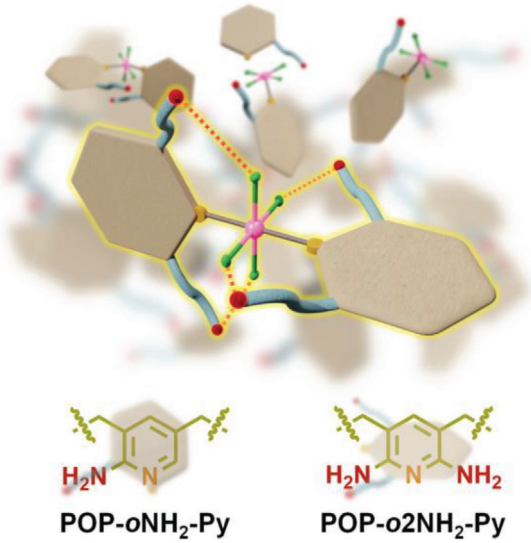

Scheme 1. Schematic illustration of tailoring coordination micro-environment in nanotraps with enhanced platinum binding affinity and the corresponding structures of aminopyridine-based POPs investigated in this study.

recovering and separating the different PGMs individually due to their similar chemical properties. Thus, developing an environmentally benign and economical method for PGM recovery and separation is highly needed. In response to this need, adsorption technology using porous materials, such as porous silica materials,[17–20] metal–organic frameworks,[21,22] and porous organic polymers (POPs),[23–26] has been studied to extract PGMs from aqueous solutions as an alternative to traditional techniques. However, current adsorbents still face challenges such as low uptake capacity, slow adsorption kinetics, limited selectivity toward target PGMs, and difficulties in material reusability. These challenges highlight the necessity for the deliberate design of the coordination micro-environment of binding sites in adsorbents to overcome these limitations.

POPs are recognized as a representative advanced porous material constructed solely from organic linkers; their building blocks can be precisely tailored by diverse functional groups, offering them plenty of opportunities for task-specific adsorbent design.[27–37] POPs also bear several advantageous features, including large surface areas, exceptional chemical and thermal stability, as well as flexible structures, which render them to be utilized in various applications with preliminary success.[38–42] Previous research in our laboratory involving palladium extraction has revealed that the addition and positioning of amino groups adjacent to the pyridine binding site significantly enhanced the nucleophilicity of palladium nanotraps, thereby improving the palladium recovery performance.[23] On the basis of the findings and outcomes from this study, an aminopyridine-based nanotrap with subtle modification was rationally designed as a customized "nanopocket", whose coordination micro-environment favors platinum over palladium, thus achieving the efficient separation of Pt/Pd in the aqueous phase (**Scheme 1**). It is important to note that our approach differs from previous reports that primarily focused on the separation of platinum and palladium using palladium-preferred adsorbents.[24] The novel POP-based adsorbent we present herein is able to selectively capture and hold platinum from a binary solution containing both platinum and palladium, thereby allowing for the collection of a pure palladium solution by separating it from the mixed PGM solution that passes through the separation column filled with our newly synthesized aminopyridine-based POP, addressing the challenge of directly obtaining pure palladium outflow from a palladium and platinum mixed solution.

2. Results and Discussion

2.1. Materials Synthesis and Characterization

To prepare the pyridine-based POPs, vinyl-functional pyridine and aminopyridine (single or double amino groups in one pyridine unit) compounds were first synthesized. The resulting monomers were subsequently dissolved in dimethylformamide (DMF) with free-radical initiator azobisisobutyronitrile (AIBN) to undergo free-radical polymerization, yielding three final polymeric materials, namely POP-Py, POP-oNH_2-Py, and POP-o2NH_2-Py, respectively, with the subtle difference in the coordination micro-environment for the comparison of palladium and platinum binding performance. Thereinto, POP-Py and POP-oNH_2-Py have been researched for extracting palladium in our previous work and would also be used for the investigation of Pt/Pd separation in the aqueous phase as the reference.[23] The transformation from the aminopyridine monomers into the respective polymers was confirmed by the solid-state ^{13}C nuclear magnetic resonance spectra (Figure S1, Supporting Information). The appearance of a strong peak at ≈32.8 ppm referred to the vinyl groups after the polymerization reaction.[43] The porosity properties of the newly synthesized POP-o2NH_2-Py were subsequently investigated through nitrogen sorption measurements collected at 77 K (Figure S2, Supporting Information), revealing that the resulting POP possesses a combination of micro- and mesopores which act as concentrated nanotraps with ample chelating sites to enable the exceptional trapping of the desired analyte, providing superior capture capabilities. The Brunauer–Emmett–Teller (BET) surface area of POP-o2NH_2-Py was calculated to be 215 $m^2\ g^{-1}$, which is approximately half the value of POP-oNH_2-Py (555 $m^2\ g^{-1}$)[44] presumably due to its denser molecular packing resulting from more confined nanospace of POP-o2NH_2-Py. The scanning electron microscopy and transmission electron microscopy (TEM) images illustrated that POP-o2NH2-Py is inherently amorphous with hierarchical porous structures, showcasing irregularly agglomerated particles with non-uniform particle sizes of a few microns (Figure S3, Supporting Information). Moreover, the resulting POP displayed discernible larger pores associated with its macropores which facilitated mass transfer.

2.2. Platinum/Palladium Sorption Studies

Inspired by the previous success of POP-Py and POP-oNH_2-Py used for palladium extraction, we first evaluated the platinum and palladium uptake capacities of all three POPs via a batch of

© 2024 Wiley-VCH GmbH

15214095, 2024, 28, Downloaded from https://onlinelibrary.wiley.com/doi/10.1002/adma.202313747 by University Of North Texas, Wiley Online Library on [30/08/2024]. See the Terms and Conditions (https://onlinelibrary.wiley.com/terms-and-conditions) on Wiley Online Library for rules of use; OA articles are governed by the applicable Creative Commons License

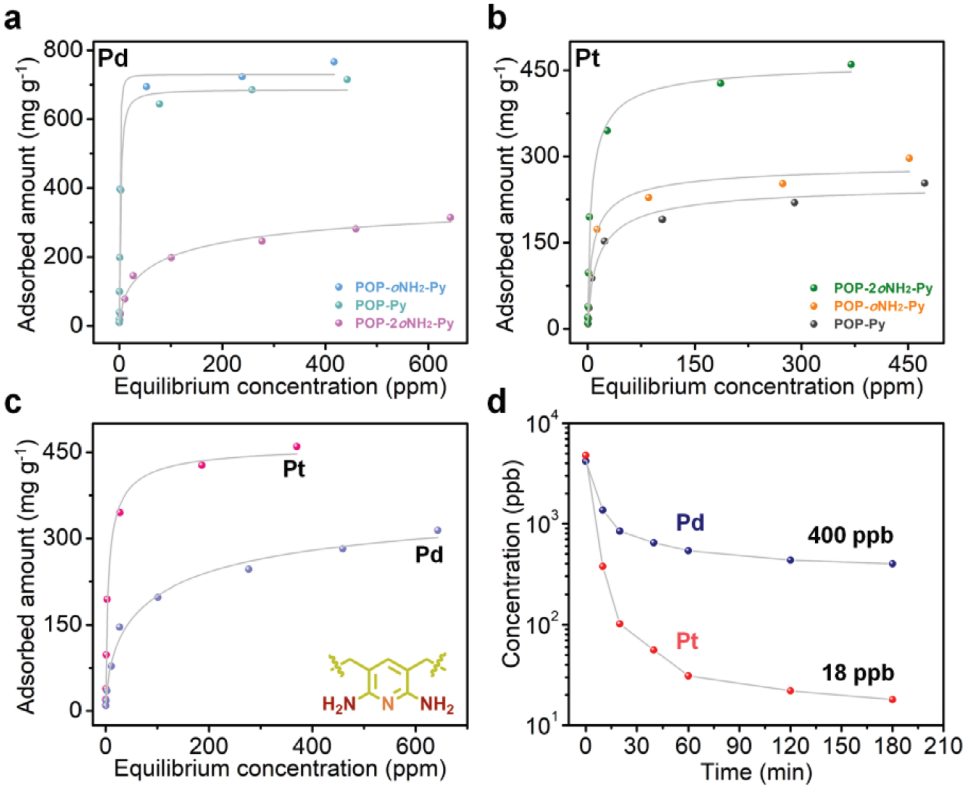

Figure 1. PGMs sorption performance evaluation. a) Palladium adsorption isotherms. b) Platinum adsorption isotherms. c) Comparison of platinum and palladium adsorption performance using POP-*o*2NH$_2$-Py. d) Kinetic performance of POP-*o*2NH$_2$-Py in platinum (red) and palladium (navy) adsorption.

adsorption experiments. To obtain the adsorption isotherms, adsorbents were treated in a set of Pd^{2+} solutions with concentrations ranging from 10–800 ppm. After contacting 12 h to achieve equilibrium, all solutions were filtered and the residual Pd^{2+} concentrations were determined by ICP. The adsorption isotherms were displayed in **Figure** 1a, POP-*o*2NH$_2$-Py was found to fit the Langmuir model, which was similar to that of POP-Py and POP-*o*NH$_2$-Py; the correlation coefficient was higher than 0.99 (Figure S4, Supporting Information). However, the uptake capacity of POP-*o*2NH$_2$-Py was only 314 mg g^{-1}, which was much lower than that of reported pyridine-based POPs, POP-Py (715 mg g^{-1}) and POP-*o*NH$_2$-Py (766 mg g^{-1}). Interestingly, the increased electron-donating ability from the extra amino group doesn't contribute to the binding affinity. The palladium adsorption performance, by contrast, is hindered by this subtle modification of the coordination micro-environment in nanotraps.

Following the palladium adsorption experiments, we then investigated the platinum adsorption performance of synthesized POPs. A sequence of solutions with increased Pt^{4+} concentrations (10–600 ppm) was prepared; an identical experimental process was used for determining the maximum capacities of all three POPs for platinum adsorption. Equilibrium platinum uptake capacity as a function of equilibrium platinum concentration is showcased in Figure 1b. Remarkably, POP-*o*2NH$_2$-Py exhibited superior platinum uptake capacities compared to both POP-Py and POP-*o*NH$_2$-Py. The introduction of additional amino groups further facilitates the binding affinity toward Pt^{4+} ions, thereby improving the overall uptake performance. As shown in Figure 1b, there is an insignificant increase in POP-*o*NH$_2$-Py (297 mg g^{-1}) for platinum adsorption compared to POP-Py (254 mg g^{-1}), whereas POP-*o*2NH$_2$-Py (460 mg g^{-1}) outperformed with more than 1.8-fold and 1.5-fold superiority to POP-Py and POP-*o*NH$_2$-Py respectively, which stands out as one of the most effective adsorbents for platinum extraction with a high uptake capacity to date, while exhibiting a high Pt/Pd uptake selectivity observed thus far as well. (**Figure** 2, Table S1, Supporting Information).[21,45–61] Typically, a lower surface area of an adsorbent could hinder adsorption performance by impeding the approach of dissolved metal ions to binding sites. However, in the case of these pyridine-based POPs for platinum adsorption, this drawback is mitigated. Accordingly, the additional incorporation of amino groups in POPs proves to be more crucial than the adsorbents' porosity in enhancing the binding affinity toward Pt^{4+} ions, consequently improving the adsorption performance. To deepen our comprehension of the adsorption mechanism of POP-*o*2NH$_2$-Py toward platinum and palladium, the BET surface area measurements of Pd/Pt@POP-*o*2NH$_2$-Py were initially conducted to ascertain the occupation of Pd and Pt ions within the absorbents' cavities. The significantly diminished surface areas of both Pd@POP-*o*2NH$_2$-Py (128 m^2 g^{-1}) and Pt@POP-*o*2NH$_2$-Py (37 m^2 g^{-1}) in comparison with raw POP-*o*2NH$_2$-Py (215 m^2 g^{-1}) indicated a decrease in the accessibility of nanotraps in adsorbents upon loading with Pd or Pt ions, verifying its strong adsorption performance for both platinum and palladium (Figure S6, Supporting Information). Powder X-ray diffraction was subsequently employed to investigate the presence of these two

© 2024 Wiley-VCH GmbH

15214095, 2024, 28, Downloaded from https://onlinelibrary.wiley.com/doi/10.1002/adma.202313747 by University Of North Texas, Wiley Online Library on [30/08/2024]. See the Terms and Conditions (https://onlinelibrary.wiley.com/terms-and-conditions) on Wiley Online Library for rules of use; OA articles are governed by the applicable Creative Commons License

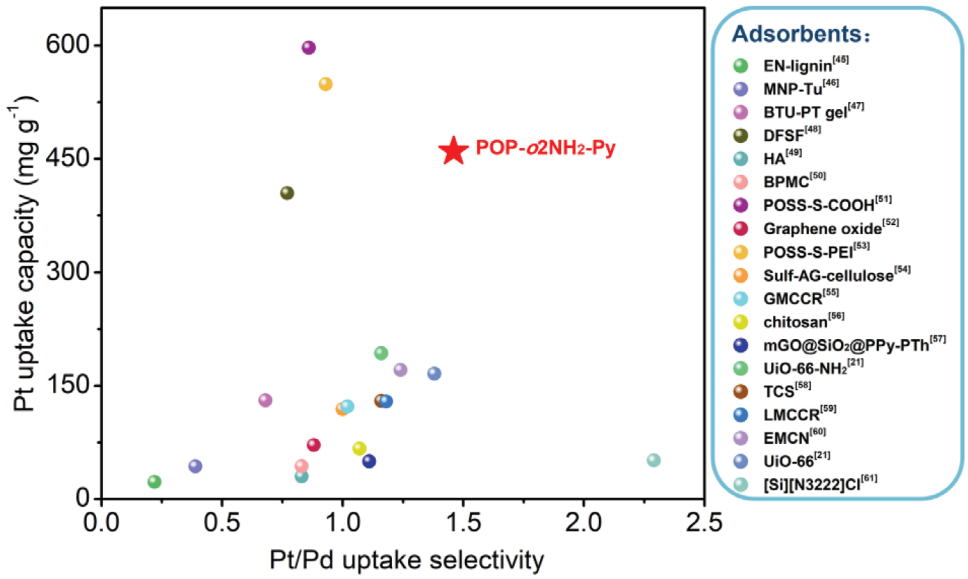

Figure 2. Comparison of platinum equilibrium uptake capacity as a function of Pt/Pd uptake selectivity of POP-*o*NH_2-Py with that of other benchmark sorbent systems (refer to detailed information of samples in Table S1, Supporting Information).

metals in the treated adsorbent samples. However, no distinguishable peaks corresponding to palladium or platinum species used in sorption experiments were detected in the loaded POP-*o*2NH_2-Py samples, indicating that the palladium and platinum ions are likely uniformly dispersed and bound within the nanotraps of POP-*o*2NH_2-Py (Figure S7, Supporting Information). High-angle annular dark-field scanning transmission electron microscopy combing with corresponding energy-dispersive X-ray analysis was additionally performed to further examine the distribution of adsorbed Pd and Pt ions in POP-*o*2NH_2-Py (Figures S8,S9, Supporting Information). These images provided clearer views into the arrangement of both Pt and Pd ions within the treated adsorbent material at the atomic level, revealing the strong binding interaction between Pt/Pd ions and POP-*o*2NH_2-Py.

Given this intriguing phenomenon and the promising outcomes observed in the selective extraction of platinum over palladium using POP-*o*2NH_2-Py (Figure 1c), further investigation was conducted to evaluate the kinetic efficiency of this adsorbent material to examine the impact of the additional amino groups on enhancing the binding affinity of the pyridine moiety toward platinum ions. 20 mg of POP-*o*2NH_2-Py was added in 200 mL of 5-ppm Pd^{2+} and Pt^{4+} solutions, respectively, 3 mL aliquots were taken out at appropriate time intervals to monitor the adsorption performance. The filtered solutions were analyzed via ICP-MS for determining the remaining Pd^{2+}/Pt^{4+} concentrations and the content of Pd^{2+}/Pt^{4+} was measured over time. Both palladium and palladium concentrations were reduced to ppb level within 20 min, and the remaining Pt^{4+} concentration in the solution was 18 ppb after 3 h, whereas the equilibrium concentration of Pd^{2+} was ≈400 ppb (Figure 1d). The time-course adsorption curves were fitted to a pseudo-second-order kinetic model (Figure S10, Supporting Information), suggesting that the rate-determining step in platinum and palladium adsorption was dominated by chemisorption. To further quantify the binding affinity of POP-*o*2NH_2-Py toward different PGMs, the distribution coefficient (K_d) was calculated at the equilibrium values (Table S2, Supporting Information). In the platinum solution, the K_d of POP-*o*2NH_2-Py (2.7×10^6 mL g^{-1}) was noted to showcase higher binding affinity by two orders of magnitude compared to that of POP-*o*2NH_2-Py (9.5×10^4 mL g^{-1}) in the palladium solution, which confirmed the contribution of extra amino groups for binding platinum ions.

2.3. Binding Mechanism Investigation

To examine the platinum and palladium binding environments within two types of aminopyridine-based POP adsorbents and to gain insight into the underlying reasons for their distinct performance on various PGMs, we investigated the samples using various spectroscopic techniques. X-ray photoelectron spectroscopy (XPS) profiles were first collected. In the XPS surveys, the strong signals of Pd 3*d* and Pt 4*f* appeared in tested POP-*o*NH_2-Py and POP-*o*2NH_2-Py, confirming that both absorbents were able to capture platinum and palladium (**Figure 3a–f**). For both Pd@POP-*o*NH_2-Py and Pd@POP-*o*2NH_2-Py, two distinct peaks observed at 343.2(1) and 337.9(8) eV corresponding to $3d_{3/2}$ and $3d_{5/2}$ in the Pd^{2+} range, verifying the presence of Pd^{2+} bound within the aminopyridine-based POPs.[62] Furthermore, the valence state of Pt in the treated POP adsorbents can also be confirmed through Pt 4*f* spectra, where doublet peaks at 76.5 ($4f_{5/2}$) and 73.2(1) ($4f_{7/2}$) eV were assigned to Pt^{4+}.[63] The variation of N 1*s* spectra of two adsorbents after loading platinum and palladium was remarkable. As shown in Figure 3a, a significant increase in the binding energy of the N 1*s* peak was observed in Pd-loaded POP-oNH_2-Py, whereas no change was found after loading platinum, indicating more charge (electron density) is transferred from the N to the Pd metal that results in a higher binding energy. On the contrary,

© 2024 Wiley-VCH GmbH

15214095, 2024, 28, Downloaded from https://onlinelibrary.wiley.com/doi/10.1002/adma.202313747 by University Of North Texas, Wiley Online Library on [30/08/2024]. See the Terms and Conditions (https://onlinelibrary.wiley.com/terms-and-conditions) on Wiley Online Library for rules of use; OA articles are governed by the applicable Creative Commons License

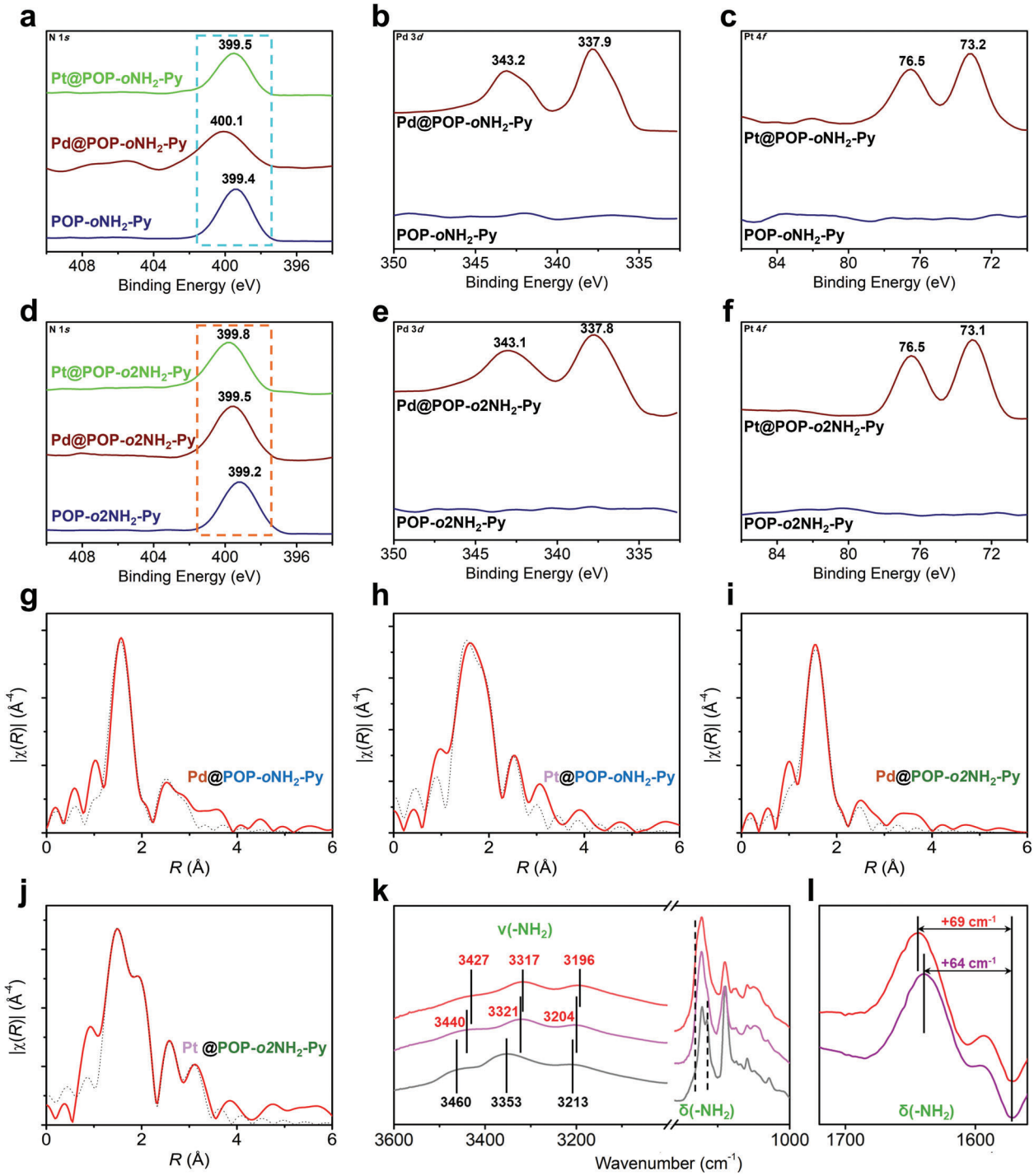

Figure 3. Binding mechanism investigation. a–c) XPS spectra of POP-*o*NH_2-Py treated by palladium or platinum. d–f) XPS spectra of POP-*o*2NH_2-Py treated by palladium or platinum. g,h) EXAFS spectra of palladium and platinum loaded POP-*o*NH_2-Py. i,j) EXAFS spectra of palladium and platinum loaded POP-*o*2NH_2-Py. k) IR spectra of pristine (gray), Pd-(purple) and Pt-(red) loaded POP-*o*2NH_2-Py, and l) shows the difference spectra in the region 1720–1560 cm^{-1} obtained by subtracting the spectrum of pristine POP-*o*2NH_2-Py from Pd-(purple) and Pt-(red) loaded one.

the N 1*s* signal in Pt-loaded POP-*o*2NH_2-Py exhibited a noticeably larger upward shift compared to the Pd-loaded sample, indicating the larger charge transfer and stronger binding between N and Pt (Figure 3d). This evidence indicated the presence of different complexation mechanisms between platinum and palladium with the dual-aminopyridine-based POP adsorbents.

To probe the coordination environment of both PGMs in the adsorbents, X-ray absorption fine structure (XAFS) spectroscopy measurement was further performed (Figure 3g–j). The results

© 2024 Wiley-VCH GmbH

15214095, 2024, 28, Downloaded from https://onlinelibrary.wiley.com/doi/10.1002/adma.202313747 by University Of North Texas, Wiley Online Library on [30/08/2024]. See the Terms and Conditions (https://onlinelibrary.wiley.com/terms-and-conditions) on Wiley Online Library for rules of use; OA articles are governed by the applicable Creative Commons License

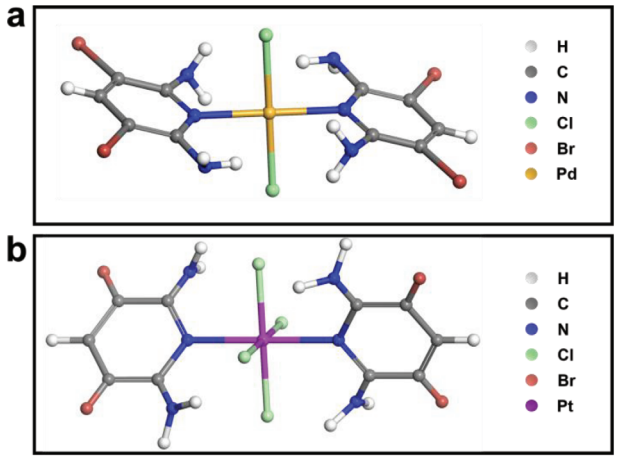

Figure 4. a) Single-crystal structures of Pd@$o2NH_2$-Py-Br and b) the DFT optimized structure of Pt@$o2NH_2$-Py-Br.

revealed that both POP-oNH_2-Py and POP-$o2NH_2$-Py demonstrated similar coordination patterns for palladium and platinum. However, the bonding between Pd and N atoms in POP-oNH_2-Py had a shorter bond length compared to the bonding between Pt and N atoms in the same adsorbent (Table S3, Supporting Information). Conversely, the Pt was found to be bound to N atoms with shorter bond lengths than Pd in POP-$o2NH_2$-Py, indicating a polar opposite binding mechanism for palladium and platinum ions compared to POP-oNH_2-Py, highlighting the distinct coordination environments of the two adsorbents. To gain more detailed structural information, attempts were made to complex the corresponding small molecular ligands with palladium and platinum salts to obtain monomeric equivalents. A single crystal of the palladium complex, named Pd@$o2NH_2$-Py-Br, was successfully obtained through the slow evaporation of a mixed water/THF solution containing Na_2PdCl_4 and the ligand (**Figure** 4a, Table S4, Supporting Information); however, efforts to crystallize Pt@$o2NH_2$-Py-Br suitable for X-ray crystallographic studies were unsuccessful. Upon mixing the $PtCl_4$ solution with the ligand solution, an instantaneous formation of a dark brown precipitate occurred, even in highly diluted solutions, suggesting that the strong binding affinity between platinum salt and the ligand impedes the formation of suitable conditions for crystal growth. Through analyzing the obtained single-crystal data, it was observed that Pd@$o2NH_2$-Py-Br exhibited a binding configuration where two pyridine units were bound to one palladium, similar to the coordination fashion observed in Pd@oNH_2-Py from our previous work.[23] Additionally, two chloride (Cl) groups were coordinated to the palladium atom, further confirming the similarity in coordination patterns between the two compounds, which also validated the EXAFS results. Based on the similar coordination modes observed in POP-$o2NH_2$-Py for both palladium and platinum through EXAFS measurements, a suggested structure for Pt@$o2NH_2$-Py-Br is presented in Figure 4b. In this proposed structure, the pyridine-based ligand maintains coordination of two, similar to the coordination observed in Pd@oNH_2-Py-Br.

The preferential capture for platinum over palladium by POP-$o2NH_2$-Py indicates that the subtle modifications introduced to its nanotraps result in a higher affinity for platinum ions. The difference in affinity can be attributed to the hydrogen bonding interactions between the amino group and the coordinated chloride ligand. In the proposed structure of Pt@$o2NH_2$-Py-Br, the four coordinated chloride ligands associated with the platinum center could form stronger intramolecular hydrogen bonds with the four amino groups in the ortho position of dual-aminopyridine ligand. In contrast, in Pd@$o2NH_2$-Py, only two chloride atoms coordinated with the palladium salt participate in the formation of intramolecular hydrogen bonding. This enhanced intramolecular hydrogen bonding contributes to the stability of the platinum complex and enables POP-$o2NH_2$-Py to selectively capture platinum over palladium. To examine the evidence of stronger intramolecular hydrogen bonding in Pt@POP-$o2NH_2$-Py, we further measured —NH_2 vibrational modes including stretching (ν) and scissoring (δ) bands using IR spectroscopy, which serve as a sensitive diagnosis for H-bond based on their frequency position,[64] similar to the well-studied H_2O vibration.[65,66] As a rule, the formation of a stronger hydrogen-bond or higher degree of the hydrogen-bonded network leads to a larger red-shift of stretching frequency and blue-shift of the scissoring frequency with respect to the free chemical group. The samples were dried under heated airflow to remove trapped moisture species, which absorb strongly at 3000–3600 cm^{-1} and thus obscure the hydrogen-bonded N—H stretching bands in this region. The dry pristine sample shows their ν(—NH_2) bands distinctly at 3460, 3353, and 3213 cm^{-1}, and δ(—NH_2) band at 1575 cm^{-1} as determined by difference spectra (Figure 3k,l).[67] In Pd and Pt@POP-$o2NH_2$-Py samples, all ν(—NH_2) bands exhibit marked red shift and δ(—NH_2) band blue shift, giving clear evidence of H-bonding formation on the amine group. More interestingly, the shift observed in Pt@POP-$o2NH_2$-Py is noticeably larger than in Pd@POP-$o2NH_2$-Py, implying that the former is subject to stronger H-bonding interaction. Such findings are supported by the DFT calculated and optimized structure model ($PdCl_2$@$o2NH_2$-Py and $PtCl_4$@$o2NH_2$-Py) in Figure S11 (Supporting Information) that shows the closer distance between Cl and H of NH_2 in Pt@POP-$o2NH_2$-Py. To further illuminate the grounds for the distinctive platinum sorption performance over palladium, the binding energies calculations for the geometry-optimized complexes were conducted as well, revealing a more compact complex of $PtCl_4$@$o2NH_2$-Py (445.8 kJ mol^{-1}) in contrast with $PdCl_2$@$o2NH_2$-Py (211.2 kJ mol^{-1}).

2.4. Selective Platinum Adsorption

Subsequently, we assessed the selective adsorption performance of the adsorbents using a binary solution containing platinum and palladium. We subjected 5 mg of the adsorbents to a 200 mL binary solution containing equal concentrations (≈50 ppm) of palladium and platinum for 12 h under stirring. In the POP-oNH_2-Py adsorption system, the platinum concentration was decreased from 43.1 to 37.7 ppm, while the remaining platinum concentration leftover upon treatment with POP-$o2NH_2$-Py was 37.1 ppm. The K_d values for platinum and palladium were calculated to study the selective platinum adsorption by POPs. The results revealed that the K_d value of POP-$o2NH_2$-Py for platinum was more than twice as high as

© 2024 Wiley-VCH GmbH

15214095, 2024, 28, Downloaded from https://onlinelibrary.wiley.com/doi/10.1002/adma.202313747 by University Of North Texas, Wiley Online Library on [30/08/2024]. See the Terms and Conditions (https://onlinelibrary.wiley.com/terms-and-conditions) on Wiley Online Library for rules of use; OA articles are governed by the applicable Creative Commons License

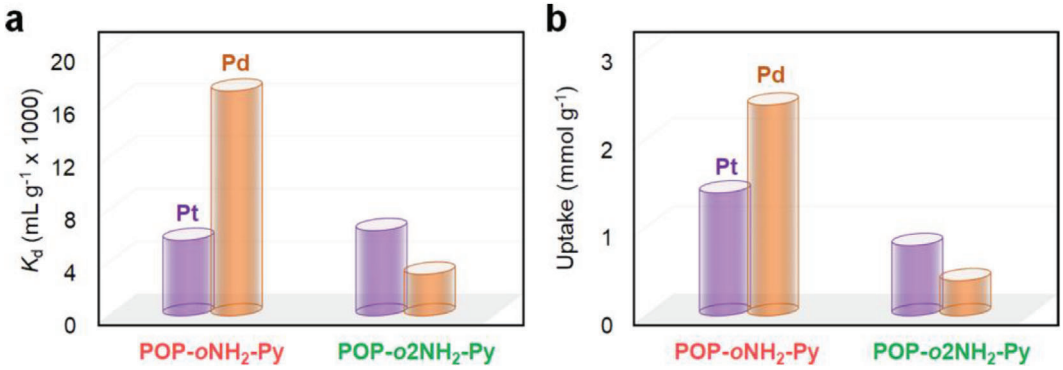

Figure 5. Pt/Pd selectivity evaluation. a) The selective adsorption performance of adsorbents was evaluated in the binary solution of platinum and palladium with equal concentrations (≈50 ppm). b) The selective adsorption performance of adsorbents was evaluated in the binary solution of platinum and palladium with equal molar concentrations (≈0.4 mM).

that for palladium (**Figure** 5a, Table S5, Supporting Information). By comparison, POP-*o*NH$_2$-Py demonstrated a higher binding affinity toward palladium than that for platinum. Furthermore, the sorption performance of aminopyridine-based POPs was assessed in the presence of equal molar concentrations of platinum (≈0.4 mM, 78.7 ppm) and palladium (≈0.4 mM, 42.8 ppm) to gain deeper insights into the superior affinity of POP-*o*2NH$_2$-Py toward platinum compared to palladium at the molecular level. The platinum uptake capacity of POP-*o*2NH$_2$-Py was measured at 0.8 mmol g^{-1} (or 156 mg g^{-1}), which was twice as high as the palladium uptake capacity (0.4 mmol g^{-1}, or 43 mg g^{-1}) (Figure 5b, Table S6, Supporting Information). On the other hand, the other adsorbent, POP-*o*NH$_2$-Py, demonstrated a preference for capturing palladium with a capacity of 2.4 mmol g^{-1} (or 255 mg g^{-1}), while its platinum uptake capacity was measured at 1.4 mmol g^{-1} (or 273 mg g^{-1}).

2.5. Breakthrough Experiments

Based on these experimental results and evidence, it can be concluded that POP-*o*2NH$_2$-Py has the potential utility for Pt/Pd separation, and the bench-scale breakthrough experiments were conducted to depict its separation performance accurately. Subsequently, dynamic breakthrough experiments were carried out on a binary mixture of platinum and palladium, with concentrations of 50 ppm each, using POP-*o*2NH$_2$-Py. The experiments were conducted in a packed 1 mL syringe containing 100 mg of the adsorbent material, under ambient conditions (**Figure** 6a). The prepared binary solution was passed through the syringe under control by a syringe pump at a rate of 10 mL hr^{-1}. As shown in Figure 6b, POP-*o*2NH$_2$-Py was able to effectively separate the equimass Pt/Pd mixtures. Following a breakthrough period of 50 min, the first liquid fraction, which exclusively contained palladium, was eluted and subsequently analyzed using

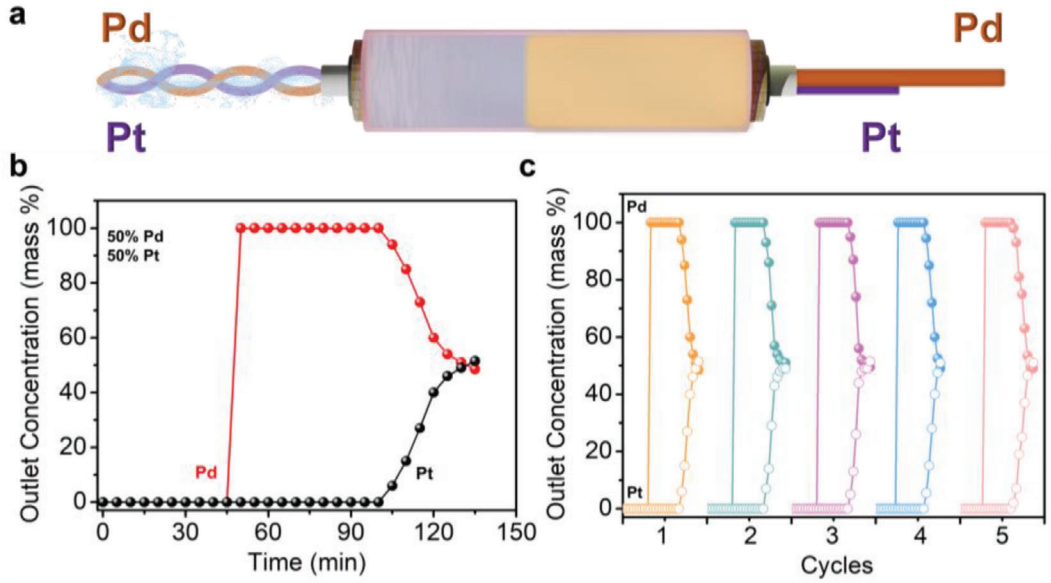

Figure 6. Breakthrough experiments. a) Schematic illustration of the breakthrough experiments. b) Experimental breakthrough curves for Pt/Pd (50/50 ppm) binary solution in a laboratory-scale separation column packing with POP-*o*2NH$_2$-Py. c) Experimental breakthrough curves for a cycling test of the Pt/Pd binary solution with the same concentrations in the separation column packing with POP-*o*2NH$_2$-Py.

© 2024 Wiley-VCH GmbH

15214095, 2024, 28, Downloaded from https://onlinelibrary.wiley.com/doi/10.1002/adma.202313747 by University Of North Texas, Wiley Online Library on [30/08/2024]. See the Terms and Conditions (https://onlinelibrary.wiley.com/terms-and-conditions) on Wiley Online Library for rules of use; OA articles are governed by the applicable Creative Commons License

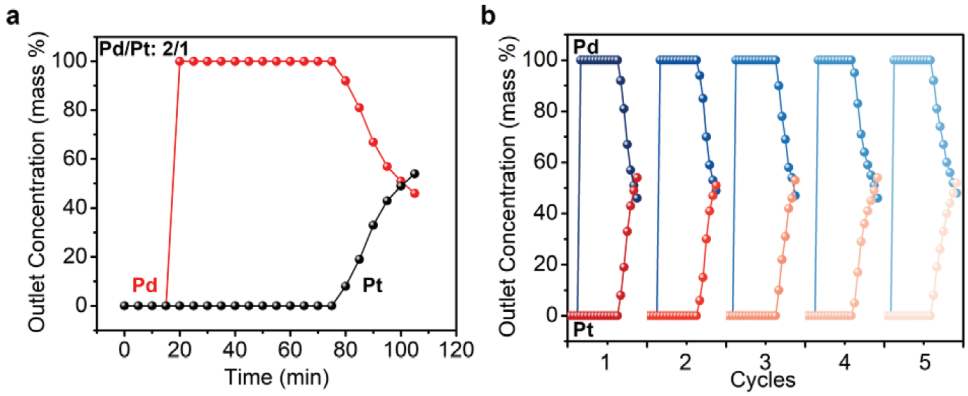

Figure 7. Breakthrough experiments in simulated TWC solution. a) Experimental breakthrough curves for Pt/Pd (50/100 ppm) solution containing competing ions Na^+ (1500 ppm), Mg^{2+} (3400 ppm), Al^{3+} (13 000 ppm), Ca^{2+} (550 ppm), and Cr^{3+} (400 ppm) in a laboratory-scale separation column packing with POP-*o*2NH_2-Py. b) Experimental breakthrough curves for a cycling test of POP-*o*2NH_2-Py using simulated TWC solution.

ICP; and rapidly it reached up to a highly pure grade without platinum outflow. This effective separation process was sustained for 55 min, providing a promising timeframe for obtaining pure palladium. The first liquid fraction containing both palladium and platinum was detected at 105 min, as the platinum uptake neared saturation, resulting in breakthrough. Considering the importance of adsorbent durability in a real-world application, the recyclability of POP-*o*2NH_2-Py was also conducted. We carried out a multicycle binary solution breakthrough experiment under identical conditions using thiourea, HCl, and NaOH solutions in sequence as eluents to flush the reacted adsorbent packed in the syringe. It is worth noting that there is no significant loss in the breakthrough time and the preferential capture of platinum persisted over five consecutive cycles (Figure 6c), confirming the promising potential of POP-*o*2NH_2-Py for Pt/Pd separation in industrial applications. Furthermore, the synthesis of POP-*o*2NH_2-Py is highly accessible, requiring only two steps for obtaining the functional monomer; and meanwhile, the polymerization of vinyl-functional monomers can be effortlessly scaled from gram to kilogram levels via easily free-radical polymerization with the assistance of a common free-radical initiator, such as AIBN. Moreover, the material economy is another crucial consideration for practical applications. The cost analysis reveals that the price of POP-*o*2NH_2-Py is ≈$37 per gram (Table S7, Supporting Information), which is comparable to other PGM adsorbents, further underscoring its suitability for real-world applications beyond the laboratory.

To evaluate the potential applicability of POP-*o*2NH_2-Py for Pd/Pt separation in a real-world scenario, cyclic breakthrough experiments for Pt/Pd separation were conducted using a custom-made simulated TWC aqueous solution in an effort to assess the PGM separation performance. The simulated TWC aqueous solution, with Pd and Pt concentrations of 100 and 50 ppm respectively, was prepared by incorporating competing metal ions including Na^+ (1500 ppm), Mg^{2+} (3400 ppm), Al^{3+} (13 000 ppm), Ca^{2+} (550 ppm), and Cr^{3+} (400 ppm), according to the metal element analysis of typical spent catalytic converters ceramic honeycomb.[68] Dynamic breakthrough experiments were then performed using these solutions, under identical experimental conditions to our bench-scale breakthrough experiments. As depicted in **Figure** 7a, Pt and Pd can be effectively separated by POP-*o*2NH_2-Py under competitive separation conditions with a breakthrough period of ≈20 min; by ≈80 min, the Pt outflow commenced from the separation column. The used adsorbent in the column was regenerated and refreshed by sequential elution with thiourea, HCl, and NaOH solutions. The separation performance of POP-*o*2NH_2-Py nearly remained after five consecutive cycles (Figure 7b), strongly demonstrating that POP-*o*2NH_2-Py possesses superior long-term stability and recyclability even in complex real-world scenarios, uncovering its significant potential as a next-generation material for PGM separation.

3. Conclusion

To conclude, we successfully developed an aminopyridine-based POP with a specifically tailored coordination micro-environment in nanotraps, which is capable of efficiently and selectively capturing platinum. Our study demonstrates that subtle modifications in the coordination micro-environment can have a significant impact on the coordination behavior of metal complexes. The dual-amino functionalized POP, POP-*o*2NH_2-Py, exhibits an opposite binding affinity toward platinum and palladium compared to its predecessor, POP-*o*NH_2-Py. Leveraging this unique adsorption model of POP-*o*2NH_2-Py, we have established a viable system for the excellent separation of Pt/Pd and high palladium productivity from binary solutions. This research presents an exciting example of a POP-based adsorbent that addresses the challenge of complex PGM separation through subtle modifications in its nanotraps, opening up new avenues for the future design of highly efficient adsorbents by finely tuning their coordination micro-environment.

[CCDC 2 283 799 contains the supplementary crystallographic data for this paper. These data can be obtained free of charge from The Cambridge Crystallographic Data Centre via www.ccdc.cam.ac.uk/data_request/cif.]

Supporting Information

Supporting Information is available from the Wiley Online Library or from the author.

© 2024 Wiley-VCH GmbH

15214095, 2024, 28, Downloaded from https://onlinelibrary.wiley.com/doi/10.1002/adma.202313747 by University Of North Texas, Wiley Online Library on [30/08/2024]. See the Terms and Conditions (https://onlinelibrary.wiley.com/terms-and-conditions) on Wiley Online Library for rules of use; OA articles are governed by the applicable Creative Commons License

Acknowledgements

This work was supported by the Robert A. Welch Foundation (B-0027). The authors also acknowledge the use of Advanced Photon Source, an Office of Science User Facility operated for the U.S. Department of Energy (DOE) Office of Science by Argonne National Laboratory and was supported by the U.S. DOE under Contract No. DE-AC02-06CH11357, and the Canadian Light Source and its funding partners. Partial support from the Researchers Supporting Project number (RSP2024R79) at King Saud University, Riyadh, Saudi Arabia is acknowledged as well.

Conflict of Interest

The authors declare no conflict of interest.

Data Availability Statement

The data that support the findings of this study are available from the corresponding author upon reasonable request.

Keywords

hydrogen bond stabilization, platinum group elements, platinum/palladium separation, porous organic polymers, tailored binding affinity

Received: December 16, 2023
Revised: April 1, 2024
Published online: May 6, 2024

[1] J. Hou, M. Yang, C. Ke, G. Wei, C. Priest, Z. Qian, G. Wu, J. Zhang, *Chem* **2020**, *2*, 100023.
[2] D. Chen, J. Zhu, Z. Pu, S. Mu, *Chem. - Eur. J.* **2021**, *27*, 12257.
[3] N. K. Chaudhari, J. Joo, H.-b. Kwon, B. Kim, H. Y. Kim, S. H. Joo, K. Lee, *Nano Res.* **2018**, *11*, 6111.
[4] P. B. Kettler, *Org. Proc. Res. Dev.* **2003**, *7*, 342.
[5] L. Osmieri, J. Park, D. A. Cullen, P. Zelenay, D. J. Myers, K. C. Neyerlin, *Curr. Opin. Electrochem.* **2021**, *25*, 100627.
[6] N. Cutillas, G. S. Yellol, C. Haro, C. Vicente, V. Rodríguez, J. Ruiz, *Coord. Chem. Rev.* **2013**, *257*, 2784.
[7] C. R. K. Rao, D. C. Trivedi, *Coord. Chem. Rev.* **2005**, *249*, 613.
[8] I. Yakoumis, M. Panou, A. M. Moschovi, D. Panias, *Clean Eng. Technol.* **2021**, *3*, 100112.
[9] W.-Q. Zhuang, J. P. Fitts, C. M. Ajo-Franklin, S. Maes, L. Alvarez-Cohen, T. Hennebel, *Curr. Opin. Biotechnol.* **2015**, *33*, 327.
[10] F. L. Bernardis, R. A. Grant, D. C. Sherrington, *React. Funct. Polym.* **2005**, *65*, 205.
[11] C. R. M. Rao, G. S. Reddi, *TrAC, Trends Anal. Chem.* **2000**, *19*, 565.
[12] B. K. Reck, T. E. Graedel, *Science* **2012**, *337*, 690.
[13] C.-H. Kim, S. I. Woo, S. H. Jeon, *Ind. Eng. Chem. Res.* **2000**, *39*, 1185.
[14] V. T. Nguyen, S. Riaño, E. Aktan, C. Deferm, J. Fransaer, K. Binnemans, *ACS Sustainable Chem. Eng.* **2021**, *9*, 337.
[15] Z. Peng, Z. Li, X. Lin, H. Tang, L. Ye, Y. Ma, M. Rao, Y. Zhang, G. Li, T. Jiang, *JOM.* **2017**, *69*, 1553.
[16] H. Dong, J. Zhao, J. Chen, Y. Wu, B. Li, *Int. J. Miner. Process.* **2015**, *145*, 108.
[17] T. Kang, Y. Park, K. Choi, J. S. Lee, J. Yi, *J. Mater. Chem.* **2004**, *14*, 1043.
[18] R. K. Sharma, A. Pandey, S. Gulati, A. Adholeya, *J. Hazard. Mater.* **2012**, *209*, 285.
[19] F. Bai, G. Ye, G. Chen, J. Wei, J. Wang, J. Chen, *Sep. Purif. Technol.* **2013**, *106*, 38.
[20] J. Kramer, N. E. Dhladhla, K. R. Koch, *Sep. Purif. Technol.* **2006**, *49*, 181.
[21] S. Lin, D. H. Kumar Reddy, J. K. Bediako, M. H. Song, W. Wei, J. A. Kim, Y. S. Yun, *J. Mater. Chem. A* **2017**, *5*, 13557.
[22] M. Zha, J. Liu, Y.-L. Wong, Z. Xu, *J. Mater. Chem. A* **2015**, *3*, 3928.
[23] B. Aguila, Q. Sun, H. C. Cassady, C. Shan, Z. Liang, A. M. Al-Enizic, A. Nafadyc, J. T. Wright, R. W. Meulenberg, S. Ma, *Angew. Chem., Int. Ed.* **2020**, *59*, 19618.
[24] K. S. Song, T. Ashirov, S. N. Talapaneni, A. H. Clark, A. V. Yakimov, M. Nachtegaal, C. Cope′ret, A. Coskun, *Chem* **2022**, *8*, 2043.
[25] Y. Bai, L. Chen, L. He, B. Li, L. Chen, F. Wu, L. Chen, M. Zhang, Z. Liu, Z. Chai, S. Wang, *Chem* **2022**, *8*, 1442.
[26] X. Yuan, Y. Wang, P. Wu, X. Ouyang, W. Bai, Y. Wan, L. Yuan, W. Feng, *Chem. Eng. J.* **2022**, *430*, 132618.
[27] Q. Sun, B. Aguila, Y. Song, S. Ma, *Acc. Chem. Res.* **2020**, *53*, 812.
[28] Y. Yue, R. T. Mayes, J. Kim, P. F. Fulvio, X.-G. Sun, C. Tsouris, J. Chen, S. Brown, S. Dai, *Angew. Chem., Int. Ed.* **2013**, *52*, 13458.
[29] W.-R. Cui, F.-F. Li, R.-H. Xu, C.-R. Zhang, X.-R. Chen, R.-H. Yan, R.-P. Liang, J.-D. Qiu, *Angew. Chem., Int. Ed.* **2020**, *59*, 17684.
[30] Y. Yuan, Q. Meng, M. Faheem, Y. Yang, Z. Li, Z. Wang, D. Deng, F. Sun, H. He, Y. Huang, H. Sha, G. Zhu, *ACS Cent. Sci.* **2019**, *5*, 1432.
[31] J. Yu, L. Yuan, S. Wang, J. Lan, L. Zheng, C. Xu, J. Chen, L. Wang, Z. Huang, W. Tao, Z. Liu, Z. Chai, J. K. Gibson, W. Shi, *CCS Chem.* **2019**, *1*, 286.
[32] X. Han, M. Xu, S. Yang, J. Qian, D. Hua, *J. Mater. Chem. A* **2017**, *5*, 5123.
[33] B. Aguila, Q. Sun, H. Cassady, C. W. Abney, B. Li, S. Ma, *ACS Appl. Mater. Interfaces* **2019**, *11*, 30919.
[34] Q. Sun, L. Zhu, B. Aguila, P. K. Thallapally, C. Xu, J. Chen, S. Wang, D. Rogers, S. Ma, *Nat. Commun.* **2019**, *10*, 1646.
[35] Y. Song, C. Zhu, Q. Sun, B. Aguila, C. Abney, L. Wojtas, S. Ma, *ACS Cent. Sci.* **2021**, *7*, 1650.
[36] Y. Hong, D. Thirion, S. Subramanian, M. Yoo, H. Choi, H. Y. Kim, J. F. Stoddart, C. T. Yavuz, *Proc. Natl. Acad. Sci. U. S. A.* **2020**, *117*, 16174.
[37] Q. Xu, X.-H. Du, D. Luo, M. Strømme, Q.-F. Zhang, C. Xu, *Chem. Eng. J.* **2023**, *458*, 141498.
[38] S. Wang, H. Li, H. Huang, X. Cao, X. Chen, D. Cao, *Chem. Soc. Rev.* **2022**, *51*, 2031.
[39] Y. Zhu, P. Xu, X. Zhang, D. Wu, *Chem. Soc. Rev.* **2022**, *51*, 1377.
[40] D.-H. Yang, Y. Tao, X. Ding, B.-H. Han, *Chem. Soc. Rev.* **2022**, *51*, 761.
[41] Y. Zhang, S. N. Riduan, *Chem. Soc. Rev.* **2012**, *41*, 2083.
[42] M. G. Mohamed, A. F. M. EL-Mahdy, M. G. Kotp, S.-W. Kuo, *Mater. Adv.* **2022**, *3*, 707.
[43] B. Aguila, Q. Sun, J. A. Perman, L. D. Earl, C. W. Abney, R. Elzein, R. Schlaf, S. Ma, *Adv. Mater.* **2017**, *29*, 1700665.
[44] Y. Song, Q. Sun, P. C. Lan, S. Ma, *ACS Appl. Mater. Interfaces* **2020**, *12*, 32827.
[45] D. Parajuli, H. Kawakita, K. Inoue, M. Funaoka, *Ind. Eng. Chem. Res.* **2006**, *45*, 6405.
[46] T.-L. Lin, H.-L. Lien, *Int. J. Mol. Sci.* **2013**, *14*, 9834.
[47] M. Gurung, B. B. Adhikari, H. Kawakita, K. Ohto, K. Inoue, S. Alam, *Ind. Eng. Chem. Res.* **2012**, *51*, 11901.
[48] Y. Harinath, N. S. Kumar, K. Seshaiah, R. Katta, D. A. Reddy, *Solid State Sci.* **2023**, *144*, 107301.
[49] D. Xue, H. Wang, Y. Liu, P. Shen, *Miner. Eng.* **2015**, *81*, 149.
[50] H. Sharififard, M. Soleimani, F. A. Ashtiani, *J. Taiwan Inst. Chem. Eng.* **2012**, *43*, 696.
[51] H. Chaudhuri, C.-R. Lim, Y.-S. Yun, *J. Mater. Chem. A* **2023**, *11*, 23463.
[52] L. Liu, S. Liu, Q. Zhang, C. Li, C. Bao, X. Liu, P. Xiao, *J. Chem. Eng. Data* **2013**, *58*, 209.
[53] H. Chaudhuri, C.-R. Lim, Y.-S. Yun, *Desalination* **2023**, *566*, 116925.
[54] M. Gurung, B. B. Adhikari, X. Gao, S. Alam, K. Inoue, *Ind. Eng. Chem. Res.* **2014**, *53*, 8565.

 © 2024 Wiley-VCH GmbH

15214095, 2024, 28, Downloaded from https://onlinelibrary.wiley.com/doi/10.1002/adma.202313747 by University Of North Texas, Wiley Online Library on [30/08/2024]. See the Terms and Conditions (https://onlinelibrary.wiley.com/terms-and-conditions) on Wiley Online Library for rules of use; OA articles are governed by the applicable Creative Commons License

[55] A. Ramesh, H. Hasegawa, W. Sugimoto, T. Maki, K. Ueda, *Bioresour. Technol.* **2008**, *99*, 3801.
[56] H. Sharififard, F. Zokaee Ashtiani, M. Soleimani, *Asia-Pac. J. Chem. Eng.* **2013**, *8*, 384.
[57] N. Jalilian, H. Ebrahimzadeh, A. A. Asgharinezhad, K. Molaei, *Microchim. Acta* **2017**, *184*, 2191.
[58] L. Zhou, J. Liu, Z. Liu, *J. Hazard. Mater.* **2009**, *172*, 439.
[59] K. Fujiwara, A. Ramesh, T. Maki, H. Hasegawa, K. Ueda, *J. Hazard. Mater.* **2007**, *146*, 39.
[60] L. Zhou, J. Xu, X. Liang, Z. Liu, *J. Hazard. Mater.* **2010**, *182*, 518.
[61] J. C. Almeida, M. C. Neves, T. Trindade, M. G. Freire, E. Pereira, *ACS Sustainable Chem. Eng.* **2024**, *12*, 442.
[62] M. Garai, M. Mahato, Y. Hong, V. Rozyyev, U. Jeong, Z. Ullah, C. T. Yavuz, *Adv. Sci.* **2021**, *8*, 2001676.
[63] F. B. Biswas, I. M. M. Rahman, K. Nakakubo, M. Endo, K. Nagai, A. S. Mashio, T. Taniguchi, T. Nishimura, K. Maeda, H. Hasegawa, *J. Hazard. Mater.* **2021**, *410*, 124569.
[64] E. Arunan, G. R. Desiraju, R. A. Klein, J. Sadlej, S. Scheiner, I. Alkorta, D. C. Clary, R. H. Crabtree, J. J. Dannenberg, P. Hobza, H. G. Kjaergaard, A. C. Legon, B. Mennucci, D. J. Nesbitt, *Pure Appl. Chem.* **2011**, *83*, 1637.
[65] T. Seki, K.-Y. Chiang, C.-C. Yu, X. Yu, M. Okuno, J. Hunger, Y. Nagata, M. Bonn, *J. Phys. Chem. Lett.* **2020**, *11*, 8459.
[66] Y. Maréchal, *The Hydrogen Bond and the Water Molecule: The Physics and Chemistry of Water, Aqueous and Bio-Media*, Elsevier, Amsterdam, The Netherlands **2007**.
[67] B. C. Smith, *Spectroscopy* **2019**, *34*, 22.
[68] I. Yakoumis, A. M. Moschovi, I. Giannopoulou, D. Panias, *IOP Conf. Ser.: Mater. Sci. Eng.* **2018**, *329*, 012009.

© 2024 Wiley-VCH GmbH

15214095, 2024, 28, Downloaded from https://onlinelibrary.wiley.com/doi/10.1002/adma.202313747 by University Of North Texas, Wiley Online Library on [30/08/2024]. See the Terms and Conditions (https://onlinelibrary.wiley.com/terms-and-conditions) on Wiley Online Library for rules of use; OA articles are governed by the applicable Creative Commons License